On the magnetic Raman scattering in $CsCoCl_3$, $CsCoBr_3$ and $RbCoCl_3$

1991 J. Phys.: Condens. Matter 3 1815

(http://iopscience.iop.org/0953-8984/3/12/012)

J. Phys.: Condens. Matter 3 (1991) 1815–1826. Printed in the UK

On the magnetic Raman scattering in $CsCoCl_3$, $CsCoBr_3$ and $RbCoCl_3$

F Matsubara, S Inawashiro and H Ohhara
Department of Applied Physics, Tohoku University, Sendai 980, Japan

Received 10 August 1990

Abstract. An analysis of the magnetic Raman scattering in quasi-one-dimensional antiferromagnets $CsCoCl_3$, $CsCoBr_3$ and $RbCoCl_3$ at the magnetically ordered regime is given. We show that discrepancies between experimental observations and the results of previous theories can be removed excellently by taking into account a next-nearest-neighbour ferromagnetic interaction J' along the c axis. We estimate the value of $J'/J = 0.1$ in those substances, where J is the nearest-neighbour antiferromagnetic interaction. Modulations of the magnetic structures for both low- and intermediate-temperature ranges are investigated by calculating the weightings of magnetic chains subject to different staggered fields. We estimate domain sizes in the modulated structures for the first time.

1. Introduction

Spin dynamics in an Ising-like $S = \frac{1}{2}$ antiferromagnet on a linear chain has been the subject of great interest for many investigators, since Villain (1975) proposed a theory of a domain-wall soliton. The compounds $CsCoCl_3$ and $CsCoBr_3$ are known to be good realization of the model and solitons in the compounds have been extensively investigated using various experimental techniques. Among them, studies of spin-wave excitations by means of magnetic Raman scattering at temperatures below the Néel temperature are very attractive, because they enable us to investigate unusual magnetic ordering (Mekata 1977, Matsubara and Ikeda 1983, Matsubara and Inawashiro 1984) in the compounds and to determine values of various physical parameters such as the intrachain and interchain exchange interactions and g-values. Breitling *et al* (1977a, b, c, 1979) first examined the spin-wave excitations in $CsCoCl_3$ by means of Raman scattering and found many discrete peaks superposed on a continuous broad peak. Very similar spectra for $CsCoBr_3$ were observed by Johnstone and Dubicki (1980). A Raman scattering study of the isomorphic compound $RbCoCl_3$ has also been made by Lockwood *et al* (1983), and a similar lineshape has been observed at lower frequencies. Shiba (1980) first explained the observations by taking into account a weak interchain interaction J_1 which yields staggered molecular fields. He showed that the staggered fields quantize the magnetic excitation continuum of the Ising-like chain, and series of discrete spectra called Zeeman ladders appear. Careful comparisons between experimental observations and calculated results were made by Lehmann *et al* (1981).

0953-8984/91/121815 + 12 $03.50

However, the following important problems have remained unsolved.

(i) Fits between experimental peak frequencies and theoretical values are not very good unless different values of the anisotropic ratio ε are chosen for the magnetic chains subject to different staggered fields. That is unacceptable from a physical point of view.

(ii) For each series of the spectra, when the peak frequency is increased, the experimental peak heights decrease more rapidly than those predicted theoretically.

(iii) A shoulder is found at the low-frequency end of the continuous spectrum.

(iv) Experimental ratios of the magnetic chains subject to staggered fields $h = 0, 2J_1$, $4J_1$ and $6J_1$ are considerably different from those predicted theoretically.

Nagler *et al* (1983) proposed an effective Hamiltonian including a slow internal staggered field h_0 from exchange mixing that influences the rapid spin fluctuations. Using the Hamiltonian, they could obtain a better fit for the peak frequency. They also pointed out that another series should appear instead of the continuous spectrum which is observed as the shoulder of the continuous spectrum, but they did not make a comparison of spectral intensities. We think that the frequency dependence of the spectral intensities is essentially the same as that obtained by Shiba and is incompatible with the experimental observations.

In this paper, we show that the discrepancies can be removed satisfactorily if we take into account the intrachain next-nearest-neighbour interaction J'. In section 2, the dynamical structure factor $S^{xx}(q, \omega)$ at the absolute zero temperature is calculated using a perturbation method. The effect of J' is studied for magnetic chains with and without a magnetic field. In section 3, comparisons of our results with experimental results for $CsCoCl_3$, $CsCoBr_3$ and $RbCoCl_3$ are made. Excellent agreement is obtained in both the peak frequency and the peak height. The values of the parameter J' are estimated for those substances together with the values of other physical parameters. We also estimate the ratios of the magnetic chains subject to different molecular fields and discuss the spin structure of the compounds. We estimate the size of domains for the first time. The results are summarized in section 4.

2. Dynamical structure factor $S^{xx}(q, \omega)$ at $T = 0$

We start with an effective Hamiltonian with $S = \frac{1}{2}$ on a linear chain described by

$$H = 2J \sum_i [S_i^z S_{i+1}^z + \varepsilon(S_i^x S_{i+1}^x + S_i^y S_{i+1}^y)]$$

$$- 2J' \sum_i [S_i^z S_{i+2}^z + \varepsilon(S_i^x S_{i+2}^x + S_i^y S_{i+2}^y)] - h \sum_j (-1)^j S_j^z$$

$$= H_{zz} + H_{xy} + H' \tag{2.1}$$

where h is the effective field from neighbouring chains. Here, $\varepsilon \ll 1$, $|J'| \ll J$, $N \gg 1$ and the periodic boundary condition is assumed.

The ground state of H_{zz} is doubly degenerate and consists of two Néel states $|N_1\rangle$ and $|N_2\rangle$ related by a spin reversal at every site. Lowest-lying excitations will occur around the Ising energy $2J$. The relevant excited states can be obtained from a Néel state by reversing a block of ν adjacent spins so as to yield a domain-wall pair state. Since we are interested in the excitation of the soliton pair, we consider the case M_t^z $(= \Sigma_i S_i^z) = 1$. In analogy with the method of previous papers (Ishimura and Shiba 1980,

Shiba 1980, Lehmann *et al* 1981), one can analyse the dynamical properties of the model at $T = 0$. We choose a set of basis states corresponding to domain-wall pairs propagating with wavevector q:

$$|\nu, q\rangle = \frac{1}{\sqrt{N}} \sum_j \exp(iqr_j) S_j^+ \prod_{m=1}^{(\nu-1)/2} (S_{j+2m-1}^- S_{j+2m}^+) |N_1\rangle. \tag{2.2}$$

Within the restricted space, the matrix elements of H are given by

$$\langle \nu, q|H|\nu, q\rangle = \begin{cases} 2J(1+\varepsilon^2)+2J'[1-\varepsilon\cos(2qa)]+2(2\nu-1)h & \text{for } \nu = 1, N-1 \\ 2J(1+\frac{3}{2}\varepsilon^2)+4J'+2(2\nu-1)h & \text{otherwise} \end{cases} \tag{2.3}$$

for diagonal terms and

$$\langle \nu, q|H|\nu_1, q\rangle = \begin{cases} V_2 & \text{for } \nu_1 = \nu - 4 \\ V & \text{for } \nu_1 = \nu - 2 \\ V^* & \text{for } \nu_1 = \nu + 2 \\ V_2^* & \text{for } \nu_1 = \nu + 4 \\ 0 & \text{otherwise} \end{cases} \tag{2.4}$$

for off-diagonal terms, where $V = J\varepsilon[1 + \exp(2iqa)]$, $V_2 = -J\varepsilon^2[1 + \exp(4iqa)]/2$ and a is the lattice constant which is set equal to unity hereafter. Here the diagonal terms are expressed apart from the ground-state energy which is approximately given by $\lambda_g = -NJ(1 + \varepsilon^2)/2 - hN/2$.

The eigenstates and eigenvalues of the Hamiltonian in the space are readily calculated numerically. The dynamical structure factor $S^{xx}(q, \omega)$ at $T = 0$ is given by

$$S^{xx}(q, \omega) = \sum_\mu |\langle \Psi_\mu(q)|S_q^+|\Psi_g\rangle|^2 \delta(\omega - \lambda_{q,\mu}) \tag{2.5}$$

where $|\Psi_\mu(q)\rangle$ and $\lambda_{q,\mu}$ are the eigenstate and eigenvalue obtained above, $S^+(q) = 1/\sqrt{N}\,\Sigma_j \exp(iqr_j) S_j^+$, $|\Psi_g\rangle$ is the ground-state approximately given by $|\Psi_g\rangle = |N_l\rangle + (\lambda_N - H_{zz})^{-1} H_{xy}|N_l\rangle$ for $l = 1$ or 2, and λ_N is the Néel state energy. We calculate $S^{xx}(q, \omega)$ for $q = 0$ using equations (2.3)–(2.5). Before comparing the theoretical lineshape of $S^{xx}(0, \omega)$ with the experimental lineshapes, we briefly mention effect of J' for chains with both $h = 0$ and $h \neq 0$.

(i) The chain with $h = 0$. The results for $S^{xx}(0, \omega)$ for different J' are presented in figure 1. The spectrum appears in the energy range

$$2J + 4J' - 4\varepsilon J + 5\varepsilon^2 J < \omega < 2J + 4J' + 4\varepsilon J + 5\varepsilon^2 J. \tag{2.6}$$

For a fixed ε, as J' is increased, the spectral intensity strongly concentrates towards lower energies. For $\varepsilon > J'/J$, the lineshape almost depends on the ratio $J'/\varepsilon J$. When $J'/J > \varepsilon$, a sharp separate peak appears at a lower frequency in addition to a small continuous peak in the energy range of equation (2.6) (Matsubara and Inawashiro 1989).

(ii) The chain with $h \neq 0$. As shown in figure 2, the Zeeman ladder occurs. For $J' = 0$, the properties of the Zeeman ladder are known: firstly the intensity is largest for the lowest energy and it decreases almost linearly as the peak energy increases; secondly the separation in the energy is the widest between the lowest two energies and it gradually

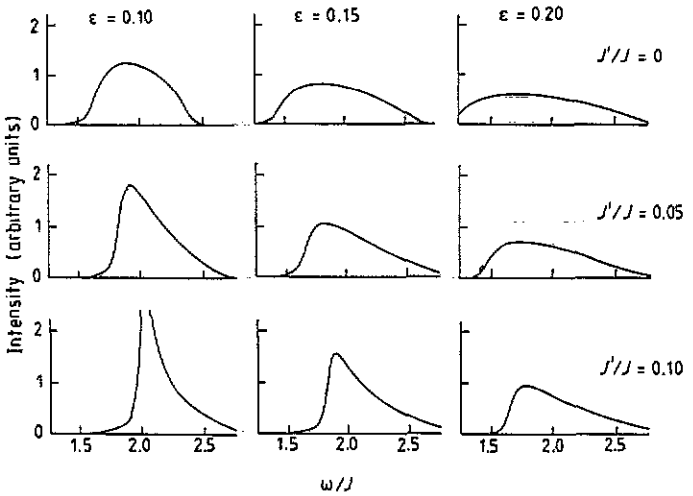

Figure 1. Continuous spectrum (C series) for different ε and J'. The spectra are convoluted with a Lorentzian lineshape of half-width 0.1 J.

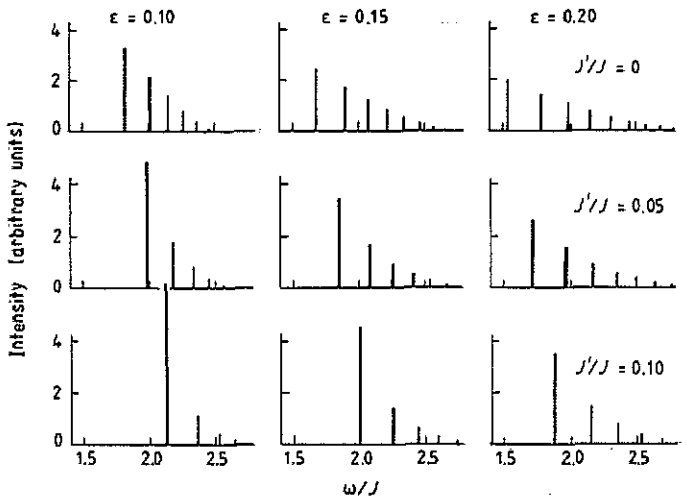

Figure 2. Zeeman ladders with $h/J = 0.02$ for different ε and J'.

decreases in a monotonic way as the energy increases. For $J' \neq 0$, these properties are pronounced. In particular, the intensity for the lowest energy is considerably larger than the others.

3. Comparison with experiments

Now we compare our results and experimental observations for $CsCoCl_3$, $CsCoBr_3$ and $RbCoCl_3$ in the magnetically ordered regime. In these compounds, the magnetic chains form a triangular array in a plane perpendicular to the chains, i.e. the c plane. In figure

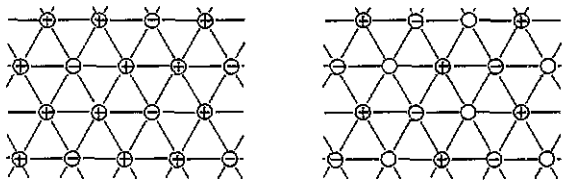

Figure 3. Postulated magnetic structures of (*a*) the FR phase at $T < T_{N2}$ and (*b*) the PDAF phase at $T_{N2} < T < T_{N1}$: +, up spins; −, down spins; ○, paramagnetic chains.

3, the postulated magnetic structures in the *c* plane are shown (Mekata 1977). At low temperatures ($T < T_{N2}$), a ferrimagnetic (FR) phase occurs owing to a very weak ferromagnetic next-nearest-neighbour interaction in the *c* plane. At intermediate temperatures ($T_{N2} < T < T_{N1}$), a partially disordered antiferromagnetic (PDAF) phase occurs owing to the frustration of the nearest-neighbour antiferromagnetic interaction in the *c* plane. The staggered fields coming from neighbouring chains take one of the four values: $h = 0, 2J_1, 4J_1$ and $6J_1$. Following Shiba (1980), we call the series of spectra arising from the magnetic chains with $h = 6J_1$, $4J_1$ and $2J_1$ the A, B_1 and B_2 ladders, respectively. We also call the continuous spectrum the C spectrum. The ratios of the magnetic chains at these different staggered fields were theoretically calculated for both spin structures (Shiba 1980). However, it has been pointed out that the magnetic structures are not stable against thermal disturbance and a kind of structure modulation occurs (Matsubara and Ikeda 1983, Matsubara and Inawashiro 1984). In fact, lines which are expected to disappear at $T < T_{N2}$ were measured by Raman scattering even at very low temperatures. Hence, analyses of the spectral intensities provide knowledge of the microscopic magnetic structure of the compounds.

The fitting parameters are J, ε, J' and J_1. The values of J, ε and J' have already been estimated by Matsubara and Inawashiro (MI) (1991) from the analyses of inelastic neutron scattering data in the paramagnetic regime obtained by Nagler *et al* (1983). Here, we estimate the values separately and compare them with the previous data to examine the validity of our model (2.1). We also fit the spectral intensities and estimate the weightings of the different magnetic chains.

3.1. $CsCoCl_3$

We first consider $CsCoCl_3$. The fitting is made by the following procedure. First, we consider the low-frequency edge of the C spectrum which is theoretically given by $\omega = 2J + 4J' - 4\varepsilon J + 5\varepsilon^2 J$. Next, we consider the energy of the zone-boundary response, $\omega = 2J + 2J'$, measured from inelastic neutron scattering (Yoshizawa *et al* 1981, Nagler *et al* 1983). Since one more condition is necessary to determine the values of the parameters, we tentatively assume $\varepsilon = 0.15$, which is obtained by MI. Thus the values of J and J' are given tentatively. Then, J_1 is given so as to fit the peak at the lowest frequency of the A ladder. Using these values, we fit the other peaks. Of course, deviations between theoretical and experimental peak positions occur at higher frequencies and minor changes in the values are made to obtain better agreement. Using the values thus

Table 1. The values of the parameters for $CsCoCl_3$ estimated by different workers.

Reference	J (K)	ε	J'/J	J_1/J
Lehmann *et al* (1981)	70.2	0.11–0.14	—	0.0125
Nagler *et al* (1983)	71.8	0.12	—	0.020
MI	62.9	0.15	0.10	—
Present work	63.6	0.145	0.095	0.0115

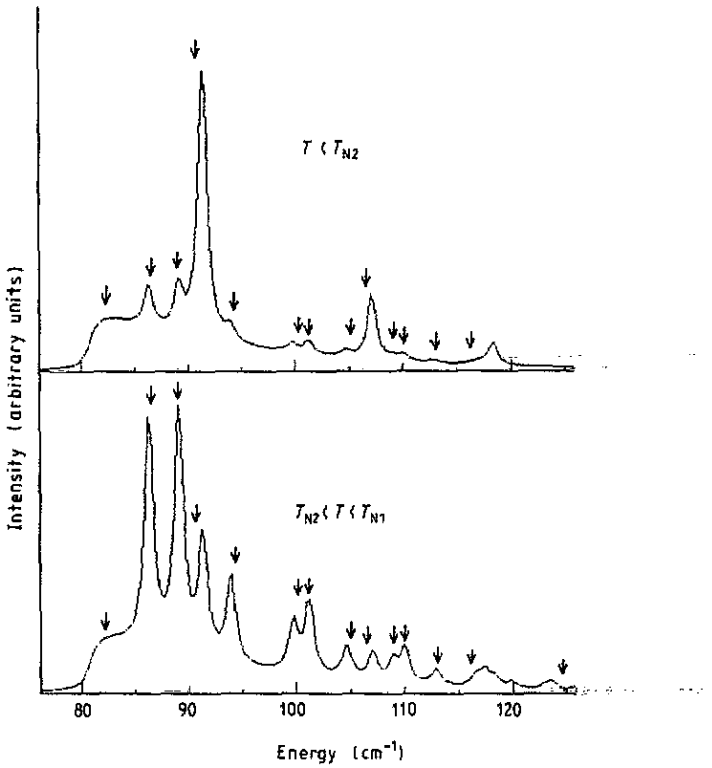

Figure 4. Calculated results for $CsCoCl_3$. The arrows indicate the experimental peak positions and the edge of the shoulder. The spectra are convoluted with a Lorentzian lineshape of the common half-width 1 cm^{-1}.

determined (table 1), we can fit all the spectra within the accuracy of 1 cm^{-1}. It should be noted that the present values agree very well with those obtained by MI, although the two sets of values are determined by different kinds of experiments.

Next, the intensities for individual peaks are calculated by using equation (2.5) and the scale factor $\bar{W}_k$ (k $\equiv$ A, B_1, B_2 and C) for each ladder is determined to fit the theoretical and experimental intensities at the lowest frequency. Using these scaling factors, $S^{xx}(0, \omega)$ is calculated and is shown in figure 4. The theoretical results reproduce the observed lineshapes very well over a wide frequency range (see figure 3 of Lehmann *et al* (1981)).

Table 2. The weighting factors (relative intensities) for $CsCoCl_3$ used to fit the spectral intensities. The theoretical values are from Shiba (1980) based on complete ordering in the FR phase and a random distribution of one-third chains in the PDAF phase.

Temperature (K)	Reference	W_A	W_{B_1}	W_{B_2}	W_C
2	Lehmann *et al* (1981)	0.37	0.07	0.18	0.41
2	Present work	0.33	0.06	0.07	0.54
2	Theory, no domain	0.33	0.00	0.00	0.67
12	Lehmann *et al* (1981)	0.10	0.29	0.43	0.14
12	Present work	0.10	0.24	0.29	0.37
12	Theory, no domain	0.08	0.25	0.25	0.42

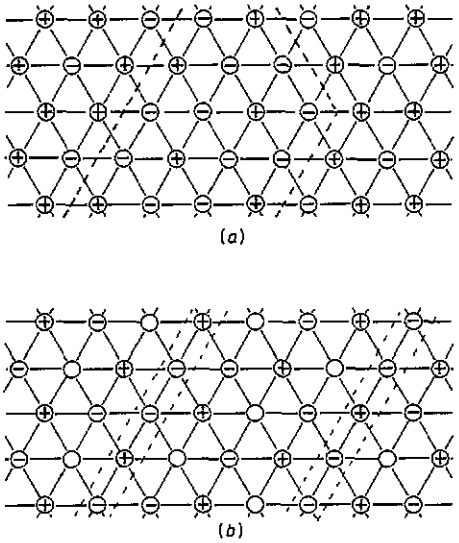

Figure 5. Schematic illustration of domains and domain walls for (*a*) $T < T_{N2}$ and (*b*) $T_{N2} < T < T_{N1}$; +, up spins; −, down spins; ○, paramagnetic chains.

The normalized scaling factors

$$W_k = \tilde{W}_k/(\tilde{W}_A + \tilde{W}_{B_1} + \tilde{W}_{B_2} + \tilde{W}_C) \tag{3.1}$$

give the ratios of the magnetic chains with the different staggered fields. Lehmann *et al* (1981) first estimated the ratios by the use of Shiba's theory. However, the ratios deviate far from those of the theoretical predictions (table 2). In particular, W_{B_2} is much larger than W_{B_1}, although both are expected to be almost the same, and W_C is much smaller than that predicted theoretically. This is a curious problem, because it suggests incompatibility between Mekata's picture of spin ordering and Shiba's theory of soliton-pair excitation, although both theories have been widely accepted. This strong discrepancy occurs because J' is neglected. Our estimation presented in table 2 gives ratios much closer to those predicted theoretically. The theoretical ratios were calculated on the

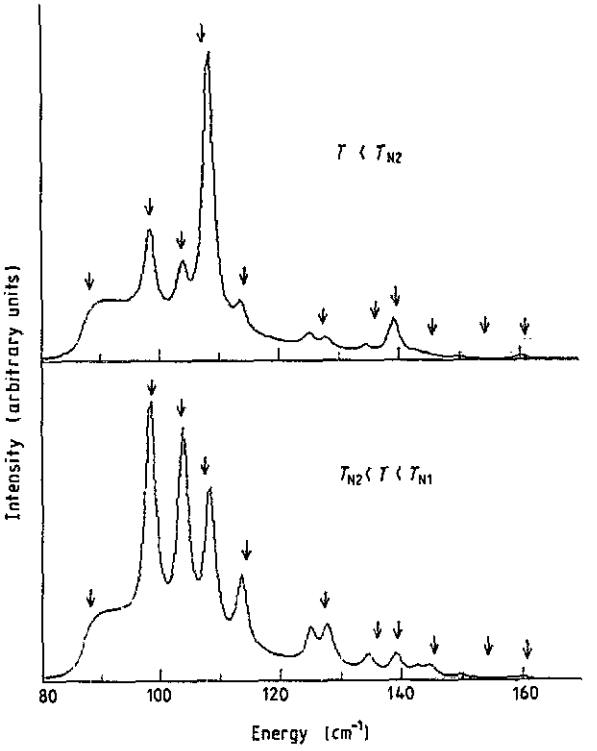

Figure 6. Calculated results for $CsCoBr_3$. The arrows indicate the experimental peak positions and the edge of the shoulder. The spectra are convoluted with a Lorentzian lineshape of common half-width 2 cm^{-1}.

assumption that the FR or PDAF magnetic structure is realized over the whole lattice. The differences between the ratios predicted theoretically and those estimated from the experimental data will arise because of the modulation of the magnetic structure due to the occurrence of domain walls.

We roughly estimate the size of the domains. We first consider the FR phase at $T < T_{N2}$. Suppose the FR domains are separated by domain walls as shown in figure 5(*a*). Here, for simplicity, we assume that the domain walls are completely shrunk and lie between lattice points. The magnetic chains away from the domain walls have a staggered field $h = 0$ or $6J_1$. On the other hand, every one-third of the magnetic chains which is adjacent to the domain walls takes the staggered field $h = 0$, $2J_1$ and $4J_1$. If we suppose that the domain wall occurs between magnetic chains with a ratio x, the ratios of the B_1 to B_2 ladders are $2x/3$. Using the obtained values of W_{B_1} and W_{B_2}, we have $x \simeq 0.1$. This means that the linear size d of the domain is about 10 in units of the lattice constant.

Next we consider the PDAF phase at $T_{N2} < T < T_{N1}$, where the domain walls have at least one magnetic chain in the unit area as shown in figure 5(*b*). In the domain walls, the ratios of the magnetic chains with $h = 0$, $2J_1$, $4J_1$ and $6J_1$ are $\frac{1}{3}$, $\frac{5}{12}$, $\frac{1}{8}$ and $\frac{1}{12}$, respectively. Hence, we can estimate the domain-wall ratio x from the difference between W_{B_1} and W_{B_2}, i.e. $(\frac{5}{12} - \frac{1}{8})x = W_{B_2} - W_{B_1}$. We obtain $x \simeq 0.2$, i.e. $d \simeq 5$.

Table 3. The values of the parameters for $CsCoBr_3$ estimated by different workers.

Reference	J (K)	ε	J'/J	J_1/J
Lehmann *et al* (1981)	90.7	0.185–0.235	—	0.019
Nagler *et al* (1983)	77.8	0.137	—	0.059
MI	69.6	0.18	0.10	—
Present work	71.2	0.17	0.10	0.026

Table 4. The weighting factors (relative intensities) for $CsCoBr_3$ used to fit the spectral intensities.

Temperature (K)	Reference	W_A	W_{B_1}	W_{B_2}	W_C
2	Lehmann *et al* (1981)	0.30	0.05	0.20	0.45
2	Present work	0.32	0.06	0.13	0.49
2	Theory, no domain	0.33	0.00	0.00	0.67
12	Lehmann *et al* (1981)	0.12	0.23	0.39	0.26
12	Present work	0.13	0.19	0.27	0.41
12	Theory, no domain	0.08	0.25	0.25	0.42

Note that this result is quite reasonable, because the system fluctuates more at higher temperatures.

Note that similar estimations of the ratio can be made from the analyses of W_A and W_C. We also estimated these ratios and obtained somewhat different values of the same order. We think that the differences come from a rough estimation of the ratios. As discussed in previous papers (Matsubara 1983, Matsubara and Inawashiro 1984), the domain walls would be very flexible and a detailed estimation of the ratios is not easy. If one can estimate the ratios by taking into account the flexibility, similar values of x will be obtained from all the ratios of W_k. We believe that the domain sizes estimated here are reliable at least in the order. It should be noted that this is the first estimation of the domain size in this compound.

3.2. $CsCoBr_3$

Next, we consider $CsCoBr_3$. The fitting procedure is the same as for $CsCoCl_3$. We only show the final results in figure 6. The values of the parameters used in the theoretical analysis are given in table 3 and the values of the ratios in table 4. As seen in figure 6, our results reproduce the peak positions and the lineshapes satisfactorily (see also figure 3 of Lehmann *et al* (1981)). The values of the parameters are also very close to those estimated by MI from the neutron scattering data of Nagler *et al* (1983). However, the deviations of the peak positions are slightly larger than in the case of $CsCoCl_3$. The deviations in the weightings are also larger than those for $CsCoCl_3$. These will be because $CsCoBr_3$ is less one dimensional and less Ising like than $CsCoCl_3$, as seen in table 3. A treatment of higher-order terms in ε as well as a more accurate treatment of the interchain interaction will be necessary to get better agreement for this compound.

Table 5. The values of the parameters for $RbCoCl_3$ estimated by different workers.

Reference	J (K)	ε	J'/J	J_1/J
Lockwood *et al* (1983)	≃70	≃0.1	—	≃0.03
Present work	71.8	0.15	0.135	0.020

Table 6. The weighting factors (relative intensities) for $RbCoCl_3$ used to fit the spectral intensities.

Temperature (K)	Reference	W_A	W_{B_1}	W_{B_2}	W_C
2.3	Present work	0.37	0.13	0.19	0.31
2.3	Theory, no domain	0.33	0.00	0.00	0.67
13.7	Present work	0.13	0.29	0.40	0.18
13.7	Theory, no domain	0.08	0.25	0.25	0.42

We also estimate the ratio x: $x \simeq 0.15$ for $T < T_{N2}$ and $x \simeq 0.32$ for $T_{N2} < T < T_{N1}$, i.e. $d \simeq 7$ for $T < T_{N2}$ and $d \simeq 3$ for $T_{N2} < T < T_{N1}$. Our results predict smaller domains in $CsCoBr_3$ than in $CsCoCl_3$. At present, it is difficult for us to discuss this problem for the reason mentioned above.

3.3. $RbCoCl_3$

The Raman spectra for this compound exhibit another interesting property. In this compound, only three prominent peaks at low frequencies are seen together with a continuous spectrum which is heavily concentrated towards lower frequencies (Lockwood *et al* 1983). We think that this results from a stronger J'. As seen in figures 1 and 2, as the ratio of $J'/\varepsilon J$ is increased, the peak at the lowest frequency grows rapidly, while the other peaks diminish. Unfortunately, it is difficult to determine values of the parameter uniquely because of a lack of the fitting points. Here, we give tentative values for them. We assume $\varepsilon = 0.15$ and J' is chosen to be not larger than εJ but close to it. Then J and J_1 are chosen to fit the theoretical and experimental peak positions. The values of the parameters obtained in this way are given in table 5 and the weights used for the fitting in table 6. In figure 7 the results of the fits between theoretical and experimental results are presented. Again, we obtain very good agreement at low frequencies. Our result predicts other peaks at high frequencies which have not been observed. At present, we do not know whether they disappear or are masked by phonon spectra at around 115 and 132 cm^{-1}.

The domain sizes of this compound are also estimated from the deviations of W_{B_1} and W_{B_2}. These are given as $d \simeq 5$ at 2.3 K, $d \simeq 3$ at 13.7 K. Our results predict further smaller domains in this compound.

4. Summary

In this paper, we have shown that the magnetic Raman scattering in $CsCoCl_3$, $CsCoBr_3$ and $RbCoCl_3$ can be excellently explained by a quasi-one-dimensional Ising-like $S = \frac{1}{2}$

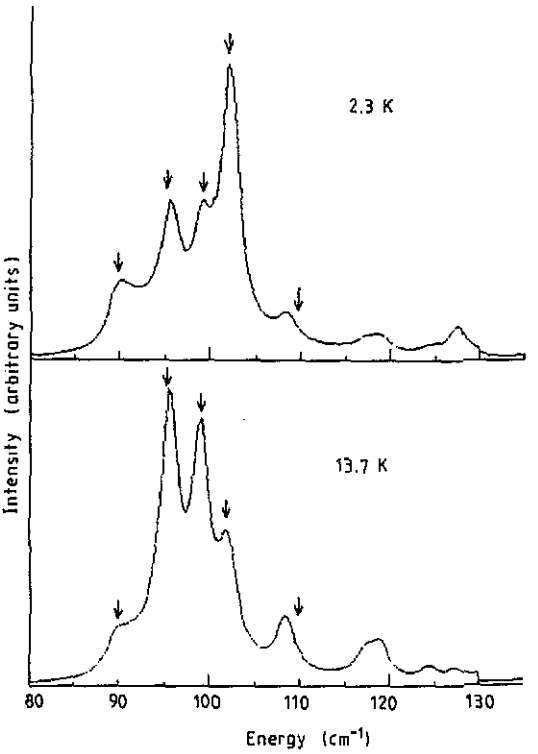

Figure 7. Calculated results for $RbCoCl_3$. The arrows indicate the experimental peak positions and the edge of the shoulder. The spectra are convoluted with a Lorentzian lineshape of common half-width 2.4 cm^{-1}.

antiferromagnet with a weak next-nearest-neighbour ferromagnetic interaction J'. We can fit not only the peak frequencies but also the peak heights excellently over a wide frequency range. The values of the parameters J, ε and J' estimated here are very close to those obtained from analyses of inelastic neutron scattering in the paramagnetic regime. We have also estimated the ratios of magnetic chains subject to different staggered fields which deviate from those predicted theoretically. We have discussed the fact that the deviations come from modulations of the magnetic structure and we estimated for the first time the domain size of the modulated structures.

The spectra for $CsCoCl_3$, $CsCoBr_3$ and $RbCoCl_3$ exhibit their own features. These have been shown to come from differences in magnitudes of ε, J'/J and J_1/J. Only when $\varepsilon \ll 1$ and J'/J is considerably smaller than ε, are the Zeeman ladders observed up to a high frequency. This is the case for $CsCoCl_3$. For $CsCoBr_3$, the system is less Ising like and the Zeeman ladders are seen up to an intermediate frequency. For $RbCoCl_3$, because of a larger J', only the prominent peaks at low frequencies are seen together with the C spectrum which is heavily concentrated at low frequencies.

It should be noted that the existence of J' in these substances suggested recently by the present authors is clearly justified by this analysis. We believe that J' also exists in other hexagonal AMX_3 compounds. The effects of J' on those compounds will be discussed separately.

References

Breitling W, Lehmann W, Srinivasan T P and Weber R 1977a *J. Magn. Magn. Mater.* **6** 116
Breitling W, Lehmann W, Srinivasan T P, Weber R and Dürr U 1977b *Solid State Commun.* **24** 267
Breitling W, Lehmann W and Weber R 1979 *J. Magn. Magn. Mater.* **10** 25
Breitling W, Lehmann W, Weber R, Leher N and Wagner V 1977c *J. Magn. Magn. Mater.* **6** 113
Ishimura N and Shiba H 1980 *Prog. Theor. Phys.* **63** 743
Johnstone I W and Dubicki K 1980 *J. Phys. C: Solid State Phys.* **13** 4531
Lehmann W, Breitling W and Weber J 1981 *J. Phys. C: Solid State Phys.* **14** 4655
Lockwood D J, Johnstone I W, Labbe H J and Briat B 1983 *J. Phys. C: Solid State Phys.* **16** 6451
Matsubara F 1983 *Solid State Commun.* **46** 329
Matsubara F and Ikeda S 1983 *Phys. Rev.* **28** 4064
Matsubara F and Inawashiro S 1984 *J. Phys. Soc. Japan* **53** 4373, and references therein
—— 1989 *J. Phys. Soc. Japan* **58** 4284
—— 1991 *Phys. Rev.* B **43** 796
Mekata M 1977 *J. Phys. Soc. Japan* **42** 76
Nagler S E, Buyers W J L, Armstrong R L and Briat B 1983 *Phys. Rev.* B **27** 1784
Shiba H 1980 *Prog. Theor. Phys.* **64** 466
Villain J 1975 *Physica* B **79** 1
Yoshizawa H, Hirakawa K, Satija S K and Shirane G 1981 *Phys. Rev.* B **23** 2298